# Restriction of Molecular Rotation and Intramolecular Charge Distribution in the Photoexcited State of Coumarin Dyes on Gold Nanoparticle Surface

**ARTICLE** *in* THE JOURNAL OF PHYSICAL CHEMISTRY C · JANUARY 2015

Impact Factor: 4.77 · DOI: 10.1021/jp510042c



**4 AUTHORS**, INCLUDING:

Tushar Debnath
Department of Atomic Energy
**17** PUBLICATIONS **55** CITATIONS
SEE PROFILE

Partha Maity
Bhabha Atomic Research Centre
**17** PUBLICATIONS **55** CITATIONS
SEE PROFILE

Hirendra N Ghosh
Bhabha Atomic Research Centre
**127** PUBLICATIONS **3,843** CITATIONS
SEE PROFILE

THE JOURNAL OF PHYSICAL CHEMISTRY C

Article

pubs.acs.org/JPCC

# Restriction of Molecular Rotation and Intramolecular Charge Distribution in the Photoexcited State of Coumarin Dyes on Gold Nanoparticle Surface

Jayanta Dana, Tushar Debnath, Partha Maity, and Hirendra N. Ghosh*

Radiation and Photochemistry Division, Bhabha Atomic Research Centre, Mumbai, 400085, India

Supporting Information

**ABSTRACT:** Effect of molecular structure on the excited state dynamics, molecular rotation, and intramolecular charge distribution in the excited states of two structurally similar coumarin dyes, namely, coumarin 343 (C-343) and 7-diethyl amino coumarin 3-carboxylic acid (D-1421), on the Au nanoparticle (NP) surface has been investigated using steady state and time-resolved emission spectroscopy. In the first excited state ($S_1$), both the coumarin dyes exist as a locally excited (LE) state in nonpolar solvent; however, in polar solvent, C-343 exists as intramolecular charge transfer (ICT) state and D-1421 predominantly exists as a twisted intramolecular charge transfer (TICT) state. Photoexcited C-343 molecules transfer energy to Au NP in aqueous solution; however, photoexcited D-1421 molecules do not transfer energy to Au NP due to poor overlap between emission band of D-1421 and plasmon absorption band of Au NP. Interestingly, emission intensity of the $S_1$ state of D-1421 drastically increases on the Au NP surface due to restriction of amino-group rotation which is responsible for the population of TICT states. Intramolecular charge distribution in the excited states for both C-343 and D-1421 dyes found to be restricted on Au NP surface.

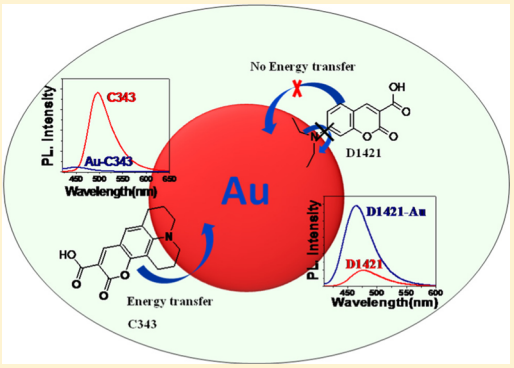


## 1. INTRODUCTION

The interactions between molecular adsorbates and metal nanoparticles (NPs) have attracted tremendous attention due to their wide applications in optical material, biosensing, scanning probe microscopy etc[1−6] and plasmonic solar cell.[7−9] Coupling between molecular resonance and surface plasmon of metal NPs is an important parameter that is found to be strongly dependent on the spectral overlap between the molecular emission and absorption of the surface plasmon.[10−13]

The fluorophore molecules optically interact with gold NPs due to their strong surface plasmon resonance. The cause of strong surface plasmon resonance is the collective oscillation of conduction band electron on metal NP surface.[14] To improve the efficiency of any device made out of these fluorophore−metal NP composite, it is important to know their interaction in both ground and excited states. It is reported in the literature that both enhancement and quenching of emission intensity of fluorophore strongly depend on size and shape of the quencher gold NPs, the orientation of fluorophore dipole moment, and overlap between emission spectrum of fluorephore and absorption spectrum of surface plasmon of gold NPs.[15−17]

It is widely reported in the literature that in dye/Au NP composite systems emission quenching of fluorophores take place mainly due to Forster Resonance Energy Transfer (FRET)[18−24] and nonradiative electron transfer from photo-excited dye molecules to Au NP.[25−27] In addition to that, recently Strouse and co-workers[28] have demonstrated surface energy transfer (SET) between Au NP and an emitting dipole (dye molecules). High molar extinction coefficient and broad bandwidth make Au NP a better fluorescence quencher.[18,19] In FRET, energy goes from an excited dye molecule (donor) to metal NP (acceptor) surface through dipole−dipole interactions.[18−20] The energy transfer process strongly depends on the degree of overlap between absorption spectrum of quencher and emission spectrum of donor molecule. It has been observed that energy transfer efficiency changes with polarity, viscosity, and pH of the medium, which are responsible for the change in the excited state properties of the dye molecules.[23] However, there is no report in the literature on how molecular orientation in the excited state of dye molecules affects the energy transfer to the metal NP.

Molecular structure and orientation of fluorophores on the NP surface are very important factors for both electron and energy transfer processes on semiconductor and metal NP surfaces. In our earlier investigation,[29−32] we have demonstrated the effect of molecular structure of coumarin dyes on interfacial electron transfer reaction on both $TiO_2$ and $ZrO_2$ NPs. It has been observed that molecules which exist as twisted intramolecular charge transfer (TICT) state in the excited state in high polar solvent are better sensitizer for dye/$TiO_2$ composite materials.[29−31] It has also been observed that TICT states facilitate interfacial charge separation and slow

Received: October 4, 2014
Revised: January 1, 2015
Published: January 2, 2015





DOI: 10.1021/jp510042c
J. Phys. Chem. C 2015, 119, 2046−2052

down back electron transfer reaction. Higher charge separation was observed due to different intramolecular charge delocalization in the excited state on the semiconductor NP surface, which completely depends on the molecular structure of the chromophore molecule. However, the effect of molecular structure and charge delocalization in the excited state of dye molecule on metal NP surface are never discussed in literature. Similarly effect of molecular structure on energy transfer from photoexcited dye molecule to metal NP is also not discussed in literature.

In the present investigation, to see the effect of molecular structure on energy transfer and charge delocalization of the photoexcited dye molecules on Au NP surface C-343 and D-1421 are chosen. In C-343, the nitrogen atom lies in the ring and exists as intramolecular charge transfer (ICT) state; on the other hand, in D-1421, the nitrogen atom exists as a free rotating diethyl amino group that predominantly exists as a twisted intramolecular charge transfer (TICT) state in high polar solvents. Effect of molecular structure on the interaction of molecular absorbance of dye molecules and plasmon band of Au NP has been discussed. Charge delocalization and excited state behavior of both dye molecules on Au NP surface have been discussed. Finally, feasibility of energy transfer processes on molecular structure on NP surface has been demonstrated.

## 2. EXPERIMENTAL SECTION

**a. Materials.** Coumarin C343, Coumarin D1421, gold chloride, trisodium citrate, sodium borohydride, and cyclohexane all are purchased from Aldrich.

**b. Au NPs Synthesis.** Au NPs were synthesized after adopting modified Turkevich method.[33,34] In brief, 250 $\mu$M gold chloride and 250 $\mu$M trisodium citrate were dissolved in 50 mL of water. The reactant mixture was stirred for 5 min for complete dissolution. Color of the solution turns into light orange. After that, 1.2 mL of ice cooled sodium borohydride solution (0.01 M) was added into the stirring solution. The effective concentration of $NaBH_4$ in the reaction mixture was 235 $\mu$M. The reactant solution was stirred for 30 min for completion of the reaction. The color of the solution changed from light orange to wine red, which can be attributed to the formation of Au NPs. This Au NP solution was diluted with water for further experiments.

**c. Time Resolved Emission Spectrometer.** Time resolved fluorescence measurements were carried out using a diode laser based spectro fluorimeter from IBH (UK). The instrument works on the principle of time-correlated single photon counting (TCSPC). In the present work, a 406 nm laser pulse was used as the excitation light sources and a TBX4 detection module (IBH) coupled with a special Hamamatsu PMT was used for fluorescence detection.

## 3. RESULTS AND DISCUSSION

**a. Characterization of Au NP.** To characterize the Au NP, high resolution TEM measurement has been carried out. Figure 1A shows the TEM image of isolated well dispersed citrate capped Au NP. The average particle size of the Au NP is 7.3 ± 0.5 nm. The size distribution has been shown in Supporting Information (SI-Figure 4). Figure 1B represents the extinction spectra of Au NP in water. The localized surface Plasmon band of Au NPs has been observed at 520 nm. Concentration of Au NP has been determined from extinction spectra and size of Au

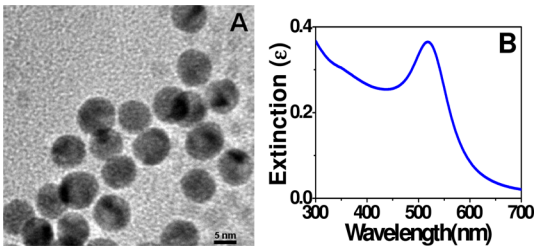


**Figure 1.** (A) High resolution TEM image of citrate stabilized Au NP. (B) Extinction spectra of Au NPs in aqueous medium.

NP after following the literature as reported by Haiss et al.[35] (see Supporting Information).

**b. Steady State Optical Absorption and Emission Studies.** Main aim of the investigation is to monitor the excited state photophysical behavior of two structurally similar coumarin molecules (C343 and D1421) on the Au NP surface and also understand the effect of dye molecules on the plasmon properties of Au NP. Before going to demonstrate the excited state behavior, it is necessary to examine the ground state interaction between these two molecules and Au NP. However, it is important to know the surface properties of Au NP before carrying out ground state interaction studies. It has already been reported in the literature[36,37] that citrate-modified Au NP is negatively charged. So, the interaction between the coumarin dyes and Au NP will take place through an amino group instead of the negatively charged carboxylic moiety (Scheme 1). At this

**Scheme 1. Schematic Diagram Showing Photoexcitation to LE States of Both C-343 and D-1421, Followed by De-Excitation to ICT States and Emission from Both LE and ICT States**[a]

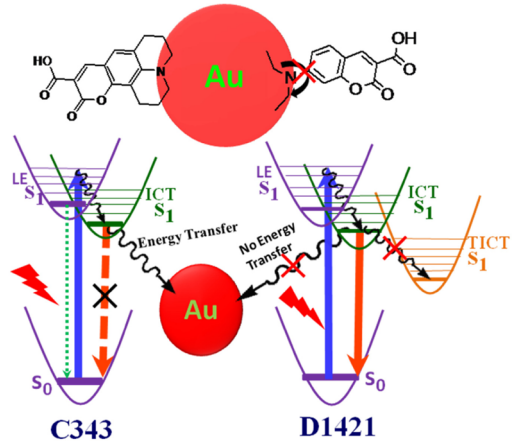


[a]In the case of C-343, energy transfer takes place from ICT states to Au NP, in addition to emission from the LE state (minor channel) due to restriction of charge delocalization. Population of TICT is completely blocked from ICT state in the case of D-1421 due to restriction of amino group rotation on the Au NP surface resulting drastic increments of ICT emission.

juncture it is very important to know the ionic charge of the coumarin dye molecules once they dissolved in water. pH of the of the aqueous solution of both C-343 and D-1421 were determined and found to be ~6. It is reported in the literature[38] that $pK_a$ values of the coumarin dyes are ~4.6. It has also been reported that at acidic pH (pH < 4) C-343 exists as the neutral protonated form. However, above pH 5 and in basic solution it


DOI: 10.1021/jp510042c
J. Phys. Chem. C 2015, 119, 2046−2052

exists as the anionic form.[38] As the pH of both coumarin dyes in water is ~6, both the coumarin dyes exist as anionic form. It has already been mentioned that the surface of the Au NP is negatively charged so both dye molecules will be attached with Au NP through an amino group.

In our earlier investigation[29,30] and in Supporting Information we have reported photophysical properties of both C-343 and D-1421. Figure 1a shows the optical absorption spectra of citrate-stabilized Au NP, which has a plasmonic band at 520 nm. Figure 2b shows an optical absorption spectrum of the

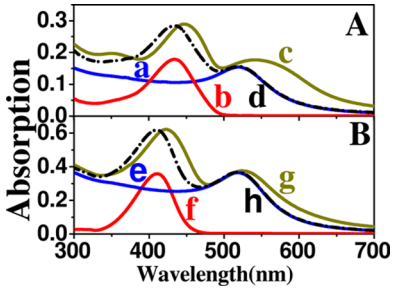


**Figure 2.** (A) Steady state optical absorption spectra of (a) Au [5.5 nM], (b) C343 [70 $\mu$M], (c) C343 [70 $\mu$M], and Au [5.5 nM] in $H_2O$; (d) addition of a and b. (B) Steady state optical absorption spectra of (e) Au [12.5 nM], (f) D1421 [100 $\mu$M], and (g) D1421 [100 $\mu$M] and Au [12.5 nm] in $H_2O$; (h) addition of e and f.

C343 molecule in water, which has an absorbance maxima at 435 nm. The composite mixture of C343/Au NP shows two absorption bands, one band at 448 nm and another broad red-shifted band at 542 nm, as shown in Figure 2c. It is clearly seen that the optical absorption peak of C-343 on the Au NP surface changes from 435 to 448 nm. On the other hand, the plasmon band (peak) of Au NP changes from 520 to 544 nm and also become broad in the presence of C-343. Figure 2B shows the optical absorption spectrum of D-1421 in the absence and in the presence of Au NP. Figure 2f shows an optical absorption spectrum of the D-1421 molecule in water, which has absorption maxima at 411 nm. Figure 2g shows the optical absorption band of the D-1421/Au NP composite, which shows two absorption bands at 433 and 527 nm, respectively.

It is interesting to see that the optical absorption band of D-1421 changes from 411 to 433 nm on the Au NP surface. Interestingly, the plasmon band of Au NP does not change much in the presence of D-1421, unlike in presence C-343. Wang and co-workers[10] have reported plasmon band of Au nanorod becomes broad and red-shifted on adsorption of dye molecules due to their strong coupling with the surface plasmon of nanorod. Earlier Karam et al.[39] also have reported the change of extinction spectra of Au nanorod after adsorbing the organic fluorophore due to molecular and plasmonic resonance coupling. It is also reported in literature that the coupling strength is found to be strongly dependent on the spectral overlap between the molecular emission and absorption of the surface plasmon.[40−42] In the present investigation it is clearly seen that in both the dye/Au NP systems optical absorption band of the coumarin dyes are red-shifted on the Au NP surface. However, it is seen that the spectral overlap between the plasmon band of Au NP and emission band of C-343 is better as compared to that of D-1421.

**c. Steady State Emission Spectroscopy of C-343 and D-1421 on the Au NP Surface.** To monitor the effect of molecular structure on molecular and plasmonic resonances in Au NP/dye interaction emission spectroscopy has been carried out for both C-343 and D-1421 in the presence of Au NP. Figure 3 shows the emission spectra of both C-343 in the

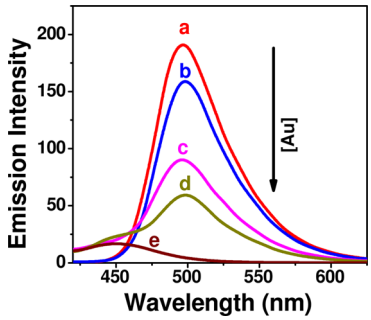


**Figure 3.** Steady state emission spectra of C-343 at different concentrations: (a) 0.0, (b) 1.5, (c) 2.5, (d) 4, and (e) 5.5 nM of Au NPs in water; [C-343] = 70 $\mu$M.

absence and in the presence of Au NP of different concentrations. C-343 shows emission maxima at 495 nm in aqueous solution. However, it has been observed that emission intensity gradually decreases on addition of Au NP. It is clearly seen that the emission intensity of C-343 at 495 nm is completely quenched in the presence of 5.5 nM Au-NP (Figure 2e). The emission quenching of C-343 in the presence of Au NP can be attributed to energy transfer from photoexcited C-343 to Au NP. Energy transfer in Au-NP/C-343 system is a viable process as emission band of C-343 overlaps with the plasmon band of Au NP (SI Figure 8). It is interesting to see that, in the presence of 5.5 nM Au NP, the emission intensity at 495 nm is completely quenched; however, a low intensity emission band is appeared at 448 nm. Now it is very important to know the nature of the emission band of C-343 at 448 nm on Au NP surface. We have shown in the Supporting Information (SI Figure 9) that C-343 has an emission band at 446 nm in cyclohexane, which is attributed to the locally excited state (LE).[29,30] The shape of the emission band of C343 on 5.5 nM Au NP surface matches quite well with emission band of C343 in cyclohexane, which arises due to the LE state emission. Thus, the emission band at 448 nm can be attributed to emission due to the LE state of C-343 on the Au NP surface. To confirm that the emission is not from Au NP, we have carried out emission spectroscopic studies of pure Au NP. No emission was observed from photoexcited Au NP. Earlier, Mattoussi and co-workers[43] have reported emission from Au nanoclusters appears to be at ~750 nm. In the present investigation, Au NP has a plasmon band at 520 nm, so the emission band at 448 nm can never be attributed to emission due to Au NP. The detailed explanation regarding the appearance of the LE state on the Au NP surface has been precisely described in the subsequent section.

Emission spectroscopy of D-1421 has also been carried out in the presence of different concentration of Au NP. Figure 4a shows the emission spectrum of D-1421 in an aqueous solution, which has an emission maxima at 475 nm. Interestingly, unlike the C-343/Au NP system, the emission intensity of D-1421 gradually increases with increasing Au NP concentration. Emission maximum of D-1421 also moves in the blue region of the spectrum with increasing Au NP concentration (Figure 4). Emission maxima of D-1421 also changes from 475 to 464 nm on Au NP surface at 12.5 nM Au NP concentration (Figure


DOI: 10.1021/jp510042c
J. Phys. Chem. C 2015, 119, 2046−2052

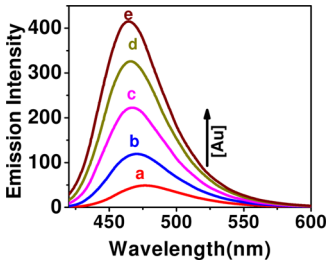


**Figure 4.** Steady state emission spectra of D1421 at different concentrations: (a) 0.0, (b) 5, (c) 8, (d) 10.5, and (e) 12.5 nM of Au NPs in water; [D-1421] = 100 $\mu$M.

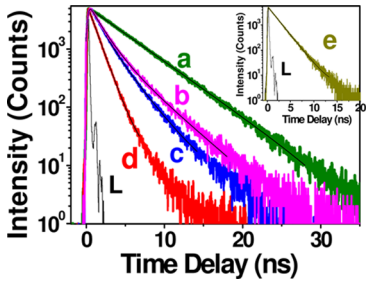


**Figure 5.** Time resolved emission decay traces of C-343 on the Au NP surface at 500 nm at different concentrations: (a) 0.0, (b) 1.5, (c) 2.5, and (d) 5.5 nM of Au NPs in water. Inset: Emission of C-343 on 5.5 nM Au NP surface at 448 nm. Excitation wavelength was kept at 406 nm. **L** stands for Lamp profile of 406 nm laser excitation source.

4e). In C343/Au NP system emission quenching was obsrved and attributed to energy transfer from photoexcited C-343 to Au NP. As the molecular structure of D-1421 is very similar to C-343, so the energy transfer from the photoexcited state of D-1421 to Au NP is also expected. However, the emission intensity of D-1421 increases with Au NP concentration, suggesting no energy transfer process is active in D-1421/Au NP system. As the emission band of D-1421 does not overlap with the plasmon band of Au NP (SI Figure 8), it is expected no energy transfer can take place in the D-1421/Au NP system. Earlier, Anger et al.[44] and Ming et al.[45] have reported that the enhancement of emission of fluorophore can take place in the presence of metal NP due to local electric field enhancement. The local field enhancement takes place when the surface plasmon band of metal nano particles lies in between the absorption band and emission band of the fluorophore. However, in D-1421/Au NP system emission band of D-1421 exists in the blue region as compared to Au NP plasmon band. Ming et al.[45] reported that maximum local field enhancement occurred when the excitation wavelength is in the center of surface plasmon band. If the excitation wavelength is in the red or blue region of the plasmon band then the local field enhancement decreases drastically. In the D-1421/Au NP system samples were excited at 400 nm so emission enhancement can not be attributed to optical enhancement. However, it is important to know the reason behind the enhancement of emission intensity of D-1421 on Au NP surface. To understand the reason for fomation of LE state for C-343 and increment of emission intensity of D-1421 on Au NP surface time-resolved emission studies have been carried out in both the systems and are described in the next section.

**d. Time-Resolved Emission Spectroscopy of C-343 and D-1421 on Au NP Surface.** To reconfirm the above-mentioned behavior of both C-343 and D-1421 on the Au NP surface, time-resolved emission measurements have been carried out after exciting the samples at 406 nm. Figure 5 shows emission decay traces of C-343 in the absence and in the presence of Au NP of different concentrations at 500 nm in water. Figure 5a depicts the emission decay kinetics of C-343 in water which can be fitted single exponentially with time constants of 4.63 ns. Interestingly in the presence of Au NP the emission kinetics decay faster and can be fitted biexponentially (Figure 5, Table 1). At 5.5 nM Au NP concentration, the emission kinetics of C-343 at 500 nm (Figure 5d) can be fitted biexponentially with time constants $\tau_1$ = 0.68 ns (6.5%) and $\tau_2$ = 1.18 ns (93.5%), with an average lifetime of 1.14 ns (Table 1). The decrement of emission lifetime on Au NP surface can be attributed to energy transfer from photoexcited C-343 to Au NP as we have mentioned earlier in steady state emission quenching studies. In steady state emission studies, we have observed C-343 shows weak intensity emission band peaking at 448 nm on Au NP at 5.5 nM concentration, which we have attributed to the LE state of C-343. The emission decay trace of C-343 at 448 nm on Au NP at 5.5 nM concentration (Figure 5e) can be fitted biexponentially with time constants $\tau_1$ = 1.15 ns (77%) and $\tau_2$ = 2.56 ns (23%), with an average lifetime of 1.74 ns. The longer component 2.56 ns can be attributed to the contribution from LE state of C-343. It has been observed that there is no overlap between LE state of C-343 and plasmon band of Au NP (SI Figure 9). As a result no energy transfer can take place from LE state of C-343 to Au NP surface. Interestingly average emission lifetime of C-343 at 448 nm on Au NP at 5.5 nM concentration (1.74 ns) is much higher as compared to that at 500 nm (1.14 ns). This observation suggests that emission at 448 nm of C-343 on the Au NP surface can be attributed to the LE state. Time-resolved emission studies have also been carried out for D-1421 in the absence and in the presence of different concentrations of Au NP in water and shown in Figure 6. It is very interesting to see that emission decay trace of D1421 in water (Figure 6a, Table 1) can be fitted biexponentially with time constants $\tau_1$ < 0.1 ns (95.6%) and $\tau_2$ = 3.38 ns (4.4%), with an average lifetime of 0.17 ns. Major emission intensity (~96%) of D-1421 decays in water with pulse-width limited time constant (<0.1 ns). Earlier Rettig et al.[46,47] reported that the photoexcited DMABEE (dimethyl amino benzoic acid ethyl ester) molecule exists as the TICT state, and it decays nonexponentially with a very short lifetime in high polar solvents. They have suggested that, on photoexcitation, such molecules are initially populated to LE or ICT state, followed by very fast relaxation to the TICT state, as nonradiative decay rates of such molecules are found to be very high. The transition from LE/ICT state to TICT has been attributed to barrierless.[47] In our earlier investigations[29,30] we have already demonstrated that, in polar solvents, the D1421 molecule exists predominantly as the TICT state. In polar solvents on excitation of the D-1421 molecule goes to the LE or ICT state and then very quickly relaxes to the TICT state through nonradiative decay. The transition from the LE/ICT state to TICT has been attributed to barrierless; as a result, we can observe the pulse width limited decay component (<0.1 ns). The long component (3.38 ns) can be attributed to the lifetime of ICT state in water. However, interestingly, on the Au NP surface with increasing NP concentration, contribution of fast component decreases and contribution of long component increases (Figure 6, Table 1). It has also been observed that the emission quantum yield of D-1421 also increases with Au NP


DOI: 10.1021/jp510042c
J. Phys. Chem. C 2015, 119, 2046−2052

**Table 1. Emission Lifetimes of C-343 and D-1421 in the Absence and in the Presence of Au NP of Different Concentrations after Exciting the Samples at 406 nm**

| $[Au\ NP]_{C343}$ | emission lifetime of C343 at 500 nm | $[Au\ NP]_{D1421}$ | emission lifetime of D-1421 at 475 nm |
|---|---|---|---|
| 0 nM | $\tau_1$ = 4.63 ± 0.2 ns | 0 nM | $\tau_1$ = 0.02 ns (96%), $\tau_2$ = 3.38 ns (4%) ($\tau_{av}$ = 0.17 ± 0.01 ns) |
| 1.5 nM | $\tau_1$ = 1.56 ns (75%), $\tau_2$ = 3.76 ns (25%) ($\tau_{av}$ = 2.12 ns ± 0.1) | 2.5 nM | $\tau_1$ = 0.19 ns (89%), $\tau_2$ = 3.16 ns (11%) ($\tau_{av}$ = 0.42 ± 0.03 ns) |
| 2.5 nM | $\tau_1$ = 1.30 ns (62%), $\tau_2$ = 2.68 ns (38%) ($\tau_{av}$ = 1.82 ± 0.1 ns) | 8 nM | $\tau_1$ = 0.14 ns (64%), $\tau_2$ = 3.4 ns (36%) ($\tau_{av}$ = 1.3 ns ± 0.05) |
| 5.5 nM | $\tau_1$ = 0.68 ns (6.5%), $\tau_2$ = 1.18 ns (93.5%) ($\tau_{av}$ = 1.14 ± 0.05 ns) | 12.5 nM | $\tau_1$ = 3.52 ± 0.2 ns |

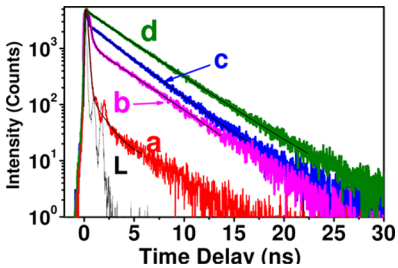


**Figure 6.** Time resolved emission decay traces of D-1421 on the Au NP surface at 475 nm at different concentrations: (a) 0.0, (b) 2.5, (c) 8, and (d) 12.5 nM of Au NPs in water. Excitation wavelength was kept at 406 nm. **L** stands for Lamp profile of 406 nm laser excitation source.

concentration. In 12.5 nM Au NP concentration, emission decay trace (Figure 6c) can be fitted single exponentially with a time constant of 3.52 ns. Therefore, at 12.5 nM Au NP concentration, the emission decay trace can be attributed to decay trace due to ICT emission. This observation clearly indicates that, on the Au NP surface, relaxation from ICT states to TICT is completely blocked.

**e. Restriction of Molecular Rotation and Charge Distribution in the Excited States of Coumarin Dyes on the Au NP Surface.** Main aim of the present investigation is to see the effect of molecular structure on the excited state dynamics and energy transfer processes on Au NP surface. Two structurally similar coumarin dyes, C-343 and D-1421, were chosen for that purpose. Steady state absorption studies suggest that the effect of molecular adsoption of C-343 on palsmon absorption of Au NP is more as compared to that of D-1421. In the presence of C-343, the plasmon absorption band of Au NP becomes broad and red-shifted (Figure 2), suggesting better interaction between C-343 and Au NP in the ground state. Steady state and time-resolved emission studies suggest that energy transfer takes place from photoexcited C-343 to Au NP. This energy transfer process can be attributed to nonradiative energy transfer (NRET), where photoexcited C-343 acts as energy donor and Au NP as energy acceptor. Nonradiative energy transfer (NRET) efficiency ($\eta$) and rate $k_{ET}$ can be calculated by using the following equations:[48]

$$\eta = 1 - \tau_{DA}/\tau_D \quad (1)$$

$$k_{ET} = 1/\tau_{DA} - 1/\tau_D \quad (2)$$

"$\eta$" and "$k_{ET}$" define the energy transfer efficiency and rate of energy transfer, respectively. $\tau_D$ and $\tau_{DA}$ represent the corresponding decay time of the donor molecule (C-343) in the absence and in the presence of acceptor (Au NP; Figure 5, Table 1). In C-343/Au NP pair, energy transfer efficiency has been calculated to be 75% and energy transfer rate to be 6.5 × $10^8$ $s^{-1}$. The most interesting part of this observation is that, at 5.5 nM Au NP concentration, emission intensity of the ICT state of C-343 is completely quenched; however, a new band appears at 448 nm, which has been attributed to the LE state of C-343. We have mentioned that the emission lifetime of C-343 at 448 nm is ∼1.74 ns. This interesting behavior of C-343 can be explained as follows. In aqueous solution, C-343 exists as the ICT state, where charge delocalization takes place between the coumarin moiety and an amino group. However, on Au NP surface majority of exited states exist as ICT states which go for energy transfer to Au NP (Scheme 1). In addition to that, on the Au NP surface, due to interference of charge delocalization, the excited state of C-343 also exists as LE state. Due to poor overlap between LE emission and Au NP plasmon band, no energy transfer can take place from LE state of C-343 to Au NP. To the best of our knowledge, this is the first example of restriction of charge delocalization of photoexcited dye molecules on the Au NP surface. Now, let us discuss the excited state behavior of D-1421 on the Au NP surface. From steady state and time-resolved emission studies it is confirmed that there is no energy transfer from photoexcited D-1421 to Au NP. However, interestingly, the emission intensity increases drastically on the Au NP surface. We have already discussed earlier and in our earlier investigation[29,30] that photoexcited D-1421 predominantly exists both as ICT state and nonemitting TICT state. Conversion of TICT state from ICT state takes place due to the rotation of a diethyl amino group in the photoexcited state of D-1421. However, the emission band appears at 475 nm can be attributed purely to the ICT state. Now, on the Au NP surface molecular rotation of the diethyl amino group of D-1421 is completely restricted, and consequently, relaxation from ICT state to TICT is completely blocked (Scheme 1). As a result, we can see the drastic increment of emission due to ICT emission of D-1421 on Au NP surface. In our earlier investigations,[29,30] we have demonstrated the effect of molecular structure on interfacial electron transfer dynamics for both C-343 and D-1421. We have shown clearly that the TICT state facilitates higher charge separation and slower back electron transfer in dye/$TiO_2$ composite materials. We would like to mention that both of the dyes coupled with $TiO_2$ nanoparticles through a carboxylic moiety result in the amino group of the coumarin dyes being free (not coupled with $TiO_2$ NP). So the excited state D-1421 can demonstrate its TICT behavior on the $TiO_2$ NP surface. However, in the present investigation, both the dye molecules are coupled with Au NP through an amino group. As a result, the excited state of D-1421 cannot demonstrate TICT behavior on the Au NP surface.

## 4. CONCLUSION

Excited state dynamics and energy transfer behavior of two structurally similar coumarin dye molecules (C-343 and D-1421) have been investigated on the Au NP surface by using steady state and time-resolved emission spectroscopy. Steady state absorption studies indicate the C-343/Au NP system has higher coupling strength between the molecular and the plasmonic resonances due to higher spectral overlap as


DOI: 10.1021/jp510042c
J. Phys. Chem. C 2015, 119, 2046−2052

compared to the D-1421/Au NP system. In nonpolar solvent both the molecules exist in the LE state, while in polar solvent, C343 exists in the ICT state and D1421 exists both in ICT and TICT states. ICT emission of C-343 was found to be quenched drastically due to energy transfer from photoexcited C-343 to Au NP. In addition to that, the excited state of C-343 also exists as the LE state on the Au NP surface due to restriction of intramolecular charge delocalization of C-343. No energy transfer could take place from photoexcited D-1421 to Au NP due to poor overlap between D-1421 emission band and Au NP plasmon absorption band. Interestingly, emission intensity of ICT state of D-1421 drastically increases on Au NP surface due to restriction of amino group rotation on NP surface. Our observation on restriction of charge delocalization of photoexcited dye molecules on NP surface opens up new phenomenon in dye-metal NP interaction. Still, further investigations in this field are necessary for in-depth understanding of the phenomenon.

## ■ ASSOCIATED CONTENT

### Supporting Information

Steady state absorption and emission and time-resolved emission studies of C-343 and D-1421 in water and in cyclohexane, HR-TEM image and size distribution of Au NP, determination of Au NPs concentration, Change of optical absorption spectra of C-343 and D-1421 with changing Au NP concentration, Emission spectra of coumarin dyes and optical absorption spectra of Au NPs, Stern−Volmer Quenching plot in C343/Au NP system. This material is available free of charge via the Internet at http://pubs.acs.org.

## ■ AUTHOR INFORMATION

### Corresponding Author

*E-mail: hnghosh@barc.gov.in. Fax: (+) 91-22-25505331/25505151.

### Notes

The authors declare no competing financial interest.

## ■ ACKNOWLEDGMENTS

This work was supported by "DAE-SRC Outstanding Research Investigator Award" (Project/Scheme No.: DAE-SRC/2012/21/13-BRNS) granted to H.N.G. J.D. and T.D. acknowledge CSIR and P.M. acknowledges DAE for research fellowship. We sincerely thank Dr. D. K. Palit and Dr. B. N. Jagatap for their encouragement.

## ■ REFERENCES

(1) Sapsford, K. E.; Berti, L.; Medintz, I. L. Materials for Fluorescence Resonance Energy Transfer Analysis: Beyond Traditional Donor-Acceptor Combinations. *Angew. Chem., Int. Ed.* **2006**, *45*, 4562−4588.

(2) Ray, P. C.; Darbha, G. K.; Ray, A.; Walker, J.; Hardy, W. Gold NP Based FRET for DNA Detection. *Plasmonics* **2007**, *2*, 173−183.

(3) Daniel, M.-C.; Astruc, D. Gold NPs: Assembly, Supramolecular Chemistry, Quantum-Size-Related Properties, and Applications Toward Biology, Catalysis, and Nanotechnology. *Chem. Rev.* **2004**, *104*, 293−346.

(4) De, M.; Ghosh, P. S.; Rotello, V. M. Applications of NPs in Biology. *Adv. Mater.* **2008**, *20*, 4225−4241.

(5) Anker, J. N.; Hall, W. P.; Lyandres, O. N.; Shah, C.; Zhao, J.; Van Duyne, R. P. Biosensing with Plasmonic Nanosensors. *Nat. Mater.* **2008**, *7*, 442−453.

(6) Fang, N.; Lee, H.; Sun, C.; Zhang, X. Sub-Diffraction-Limited Optical Imaging with a Silver Superlens. *Science* **2005**, *308*, 534−537.

(7) Atwater, H. A.; Polman, A. Plasmonics for Improved Photovoltaic Devices. *Nat. Mater.* **2010**, *9*, 205−213.

(8) Ferry, V. E.; Sweatlock, L. A.; Pacifici, D.; Atwater, H. A. Plasmonic Nanostructure Design for Efficient Light Coupling into Solar Cells. *Nano Lett.* **2008**, *8*, 4391−4397.

(9) Kulkarni, A. P.; Noone, K. M.; Munechika, K.; Guyer, S. R.; Ginger, D. S. Plasmon-Enhanced Charge Carrier Generation in Organic Photovoltaic Films Using Silver Nanoprisms. *Nano Lett.* **2010**, *10*, 1501−1505.

(10) Ni, W.; Yang, Z.; Chen, H.; Li, Li.; Wang, J. Coupling between Molecular and Plasmonic Resonances in Freestanding Dye-Gold Nanorod Hybrid Nanostructures. *J. Am. Chem. Soc.* **2008**, *130*, 6692−6693.

(11) Haes, A. J.; Zou, S. L.; Zhao, J.; Schatz, G. C.; Van Duyne, R. P. Localized Surface Plasmon Resonance Spectroscopy Near Molecular Resonances. *J. Am. Chem. Soc.* **2006**, *128*, 10905−10914.

(12) Zhao, J.; Jensen, L.; Sung, J. H.; Zou, S. L.; Schatz, G. C.; Van Duyne, R. P. Interaction of Plasmon and Molecular Resonances for Rhodamine 6G Adsorbed on Silver NPs. *J. Am. Chem. Soc.* **2007**, *129*, 7647−7656.

(13) Wurtz, G. A.; Evans, P. R.; Hendren, W.; Atkinson, R.; Dickson, W.; Pollard, R. J.; Zayats, A. V. Molecular Plasmonics with Tunable Exciton−Plasmon Coupling Strength in J-Aggregate Hybridized Au Nanorod Assemblies. *Nano Lett.* **2007**, *7*, 1297−1303.

(14) El-Sayed, M. A. Some Interesting Properties of Metals Confined in Time and Nanometer Space of Different Shapes. *Acc. Chem. Res.* **2001**, *34*, 257−264.

(15) Nakamura, T.; Hayashi, S. Enhancement of Dye Fluorescence by Gold NPs: Analysis of Particle Size Dependence. *Jpn. J. Appl. Phys.* **2005**, *44*, 6833−6837.

(16) Dong, L.; Ye, F.; Hu, J.; Popov, S.; Friberg, A. T.; Muhammed, M. Fluorescence Quenching and Photo Bleaching in Au/Rh6G nanoassemblies: Impact of Competition Between Radiative and Nonradiative Decay. *J. Eur. Opt. Soc.* **2011**, *6*, 11019−6.

(17) Thomas, K. G.; Kamat, P. V. Making Gold NPs Glow: Enhanced Emission from a Surface-Bound Fluoroprobe. *J. Am. Chem. Soc.* **2000**, *122*, 2655−2656.

(18) Huang, T.; Murray, R. W. Quenching of $[Ru(bpy)_3]^{2+}$ Fluorescence by Binding to Au NPs. *Langmuir* **2002**, *18*, 7077−7081.

(19) Forster, T. Intermolecular Energy Migration and Fluorescence. *Ann. Phys.* **1948**, *437*, 55−75.

(20) Lakowicz, J. R. *Principles of Fluorescence Spectroscopy*, 3rd ed.; Springer: New York, 2006.

(21) Dulkeith, E.; Morteani, A. C.; Niedereichholz, T.; Klar, T. A.; Feldmann, J.; Levi, S. A.; van Veggel, F. C. J. M.; Reinhoudt, D. N.; Möller, M.; Gittins, D. I. Fluorescence Quenching of Dye Molecules near Gold NPs: Radiative and Nonradiative Effects. *Phys. Rev. Lett.* **2002**, *89*, 203002.

(22) Dulkeith, E.; Ringler, M.; Klar, T. A.; Feldmann, J.; Muñoz Javier, A.; Parak, W. J. Gold NPs Quench Fluorescence by Phase Induced Radiative Rate Suppression. *Nano Lett.* **2005**, *5*, 585−589.

(23) Sen, T.; Patra, A. Recent Advances in Energy Transfer Processes in Gold-NP-Based Assemblies. *J. Phys. Chem. C* **2012**, *116*, 17307−17317.

(24) Sen, T.; Sadhu, S.; Patra, A. Surface Energy Transfer from Rhodamine 6G to Gold NPs: A Spectroscopic Ruler. *Appl. Phys. Lett.* **2007**, *91*, 043104−3.

(25) Thomas, K. G.; Kamat, P. V. Chromophore-Functionalized Gold NPs. *Acc. Chem. Res.* **2003**, *36*, 888−898.

(26) Fan, C. H.; Wang, S.; Hong, J. W.; Bazan, G. C.; Plaxco, K. W.; Heeger, A. J. Beyond Superquenching: Hyper-Efficient Energy Transfer from Conjugated Polymers to Gold NPs. *Proc. Natl. Acad. Sci. U.S.A.* **2003**, *100*, 6297−6301.

(27) Kamat, P. V.; Barazzouk, S.; Hotchandani, S. Electrochemical Modulation of Fluorophore Emission at a Nanostructured Gold Film. *Angew. Chem., Int. Ed.* **2002**, *41*, 2764−2767.

(28) Breshike, C. J.; Riskowski, R. A.; Strouse, G. F. Leaving Förster Resonance Energy Transfer Behind: Nanometal Surface Energy Transfer Predicts the Size-Enhanced Energy Coupling between a



DOI: 10.1021/jp510042c
J. Phys. Chem. C 2015, 119, 2046−2052

Metal NP and an Emitting Dipole. *J. Phys. Chem. C* **2013**, *117*, 23942−23949.
(29) Ramakrishna, G.; Ghosh, H. N. Efficient Electron Injection from Twisted Intramolecular Charge Transfer (TICT) State of 7-Diethyl Amino Coumarin 3-Carboxylic Acid (D-1421) Dye to $TiO_2$ NP. *J. Phys. Chem. A* **2002**, *106*, 2545−2553.
(30) Verma, S.; Ghosh, H. N. Tuning Interfacial Charge Separation by Molecular Twist: A New Insight into Coumarin Sensitized $TiO_2$ Film. *J. Phys. Chem. C* **2014**, *118*, 10661−10669.
(31) Debnath, T.; Maity, P.; Lobo, H.; Singh, B.; Shankarling, G. S.; Ghosh, H. N. Extensive Reduction in Back Electron Transfer Reaction in Newly Synthesized Twisted Intramolecular Charge Transfer (TICT) Coumarin Dye Sensitized $TiO_2$ NPs/Film: A Femtosecond Transient Absorption Study. *Chem.—Eur. J.* **2014**, *20*, 3510−3519.
(32) Ramakrishna, G.; Singh, A. K.; Palit, D. K.; Ghosh, H. N. Electron Transfer Dynamics of 7-*N*,*N*-Dimethyl Coumarin 4-Acetic Acid (DMACA) and 7-Hydroxy Coumarin 4-Acetic Acid (HCA) into $TiO_2$ and $ZrO_2$ NPs. *J. . Phys. Chem. B* **2004**, *108*, 12489−12496.
(33) Enüstün, B. V.; Turkevich, J. Coagulation of Colloidal Gold. *J. Am. Chem. Soc.* **1963**, *85*, 3317−3328.
(34) Kimling, J.; Maier, M.; Okenve, B.; Kotaidis, V.; Ballot, H.; Plech, A. Turkevich Method for Gold NP Synthesis Revisited. *J. Phys. Chem. B* **2006**, *110*, 15700−15707.
(35) Haiss, W.; Thanh, N.T. K.; Aveyard, J.; Fernig, D. G. Determination of Size and Concentration of Gold NPs from UV/Vis Spectra. *Anal. Chem.* **2007**, *79*, 4215−4221.
(36) Brewer, S. H.; Glomm, W. R.; Johnson, M. C.; Knag, M. K.; Franzen, S. Probing BSA Binding to Citrate-Coated Gold NPs and Surfaces. *Langmuir* **2005**, *21*, 9303−9307.
(37) Chithrani, B. D.; Ghazani, A. A.; Chan, W. C. W. Determining the Size and Shape Dependence of Gold NP Uptake into Mammalian Cells. *Nano Lett.* **2006**, *6*, 662−668.
(38) Riter, R. E.; Undiks, E. P.; Levinger, N. E. Impact of Counterion on Water Motion in Aerosol OT Reverse Micelles. *J. Am. Chem. Soc.* **1998**, *120*, 6062−6067.
(39) Karam, T. E.; Haber, L. H. Molecular Adsorption and Resonance Coupling at the Colloidal Gold NP Interface. *J. Phys. Chem. C* **2014**, *118*, 642−649.
(40) Haes, A. J.; Zou, S. L.; Zhao, J.; Schatz, G. C.; Van Duyne, R. P. Localized Surface Plasmon Resonance Spectroscopy near Molecular Resonances. *J. Am. Chem. Soc.* **2006**, *128*, 10905−10914.
(41) Zhao, J.; Jensen, L.; Sung, J. H.; Zou, S. L.; Schatz, G. C.; Van Duyne, R. P. Interaction of Plasmon and Molecular Resonances for Rhodamine 6G Adsorbed on Silver NPs. *J. Am. Chem. Soc.* **2007**, *129*, 7647−7656.
(42) Wurtz, G. A.; Evans, P. R.; Hendren, W.; Atkinson, R.; Dickson, W.; Pollard, R. J.; Zayats, A. V. Molecular Plasmonics with Tunable Exciton−Plasmon Coupling Strength in J-Aggregate Hybridized Au Nanorod Assemblies. *Nano Lett.* **2007**, *7*, 1297−1303.
(43) Aldeek, F.; Ji, X.; Mattoussi, H. Quenching of Quantum Dot Emission by Fluorescent Gold Clusters: What It Does and Does Not Share with the Forster Formalism. *J. Phys. Chem. C* **2013**, *117*, 15429−15437.
(44) Anger, P.; Bharadwaj, P.; Novotny, L. Enhancement and Quenching of Single-Molecule Fluorescence. *Phys. Rev. Lett.* **2006**, *96*, 113002.
(45) Ming, T.; Chen, H.; Jiang, R.; Li, Q.; Wang, J. Plasmon-Controlled Fluorescence: Beyond the Intensity Enhancement. *J. Phys. Chem. Lett.* **2012**, *3*, 191−202.
(46) Lippert, E.; Rettig, W.; Bonacic-Koutecky, V.; Heisel, F.; Miehe, J. A. Photophysics of Internal Twisting. *Adv. Chem. Phys.* **1987**, *68*, 1−174.
(47) Rettig, W.; Wermuth, G. J. The Kinetics of Formation of Twisted Intramolecular Charge Transfer (TICT) States in *p*-substituted Dialkylanilines: Consequences of Conical Intersections along the Reaction Coordinate. *Photochemistry* **1985**, *28*, 351−366.
(48) Főrster, T. Transfer Mechanisms of Electronic Excitation. *Discuss. Faraday Soc.* **1959**, *27*, 7−17.


DOI: 10.1021/jp510042c
*J. Phys. Chem. C* 2015, 119, 2046−2052